Precise Photometry of Transits and Occultations of the Exoplanet WASP-12b

Mikael Ingemyr

under the direction of
Prof. Joshua N. Winn
Department of Physics
Kavli Institute of Astrophysics and Space Research
Massachusetts Institute of Technology

Research Science Institute
July 27, 2010

Abstract

This paper presents precise photometric observations of transits as well as occultations of the exoplanet WASP-12b using the 1.2m telescope at Fred Lawrence Whipple Observatory and the 2.56m Nordic Optical Telescope at Roque de los Muchachos Observatory. Transits were observed in z'-band and V-band respectively and an MCMC algorithm constrained the radius to $1.82^{+0.12}_{-0.10}\ R_j$. This confirms the bloated radius reported by Hebb et al.[7] (2009) and consolidates WASP-12b as the largest planet known to date. The occultations of WASP-12b were detected in i'-band with 9σ confidence. A drop in flux of $0.046^{+0.005}_{-0.005}\%$ was measured centered at phase $\phi = 0.518^{+0.003}_{-0.004}$, consistent an orbital eccentricity of $|e\cos\omega| = 0.027^{+0.006}_{-0.005}$. The result is consistent with the z'-band detection reported by Lopez-Morales et al.[16] (2010). The observed eccentricity could explain the large size through tidal heating.

Summary

This paper presents precise measurements of the exoplanet WASP-12b undergoing transit in front of its host star and being occulted by its host star. The observations were made in different broadband wavelength filters using the 1.2m telescope at Fred Lawrence Whipple Observatory and the 2.56m Nordic Optical Telescope at Roque de los Muchachos Observatory. It is confirmed through the transit observations that WASP-12b is indeed one of the largest and most bloated planets known, perhaps even the largest. The observations of the occultations suggests that WASP-12b has a slightly eccentric orbit. The eccentricity could explain the bloated size of WASP-12b through tidal heating effects.

1 Introduction

Ever since the very first planet orbiting a sun-like star outside of our solar system was discovered by M. Mayor and D. Queloz[15] in 1995, the number of extrasolar planets discovered has increased exponentially. Their diversity provide a vast resource of information on the properties of other planets, including planetary size, mass, proximity to their host stars, orbital eccentricity, atmospheric composition and even clues about the formation and evolution of planetary systems (J. N. Winn[22]).

There are many methods used to discover and measure the properties of extrasolar planetary systems. The most successful method to date is to measure the radial velocity of stars by spectroscopy, seeking sinusoidal variations that might be caused by gravitational interactions with a second or more bodies. Such observations can give lower bounds on the mass of the other bodies, given that the mass of the star is known through stellar models, and give a value of the eccentricity e of the orbit, when fitting a Keplerian orbital motion to the radial velocity data. One constraint for determining the eccentricity with Doppler spectroscopy is that a Keplerian orbit can never get more circular than $e = 0$. Any noise or uncertainty in the measurement will inherently lead to a small eccentricity in the best-fit orbit, even for an orbit that is actually circular (Husnoo et al.[8] 2010). Another, more direct, way of determining the eccentricity of the orbit of a planet is to measure the duration and time of the transit together with the occultation (Kallrath & Milone[10] 1999). If an orbit is circular, the occultation occurs at exactly phase 0.5 and has the same duration as the transit. The problem with such an approach is that the occultation is inherently difficult to measure, since it is between one to two orders of magnitude less distinct than the transit (Lopez-Morales et al.[16] 2010).

Our understanding of planetary systems has been challenged many times by new discoveries the last decades. Among the more surprising early discoveries made using Doppler

spectroscopy was the detection of so-called hot Jupiters, large gaseous planets orbiting very close to their host stars, which was very unexpected (Mayor & Queloz[15] 1995). The nowadays large class of exotic planets has had significant impact on the modeling and theory about how solar and planetary systems form and evolve over time. The transit observations of HD209458b, the first known transiting extrasolar planet, made it possible to determine its size, and it was found to have a radius 30% greater than that of Jupiter (Charbonneau et al.[3] 2000), which contradicted the standard evolutionary models on how large a radius planets of that age should have (Knutson et al.[11] 2007; Burrows et al.[1] 2007). It is therefore said to be bloated, or inflated, and many other planets whose radii tend to be similarly difficult to explain by standard planetary models have been discovered since then, including the very-hot Jupiter WASP-12b (Hebb et al.[7] 2009) with a radius over 40% larger than predicted by today's standard planetary models.

Ibgui et al.[9] (2010) and Miller, Fortney & Jackson[17] (2009) have proposed that tidal heating effects due to a non-zero eccentric orbit explains the inflated radii of some hot Jupiters, such as WASP-12b. One constraint for such an explanation is that the very close-in orbits of some inflated hot Jupiters should quickly circularize themselves (Rasio et al.[20] 1996). The bloated radius of WASP-12b is difficult to explain if the orbit is circular (Li et al.[13] 2010). Measuring the eccentricity is thus key to testing all of these models.

The WASP-12b discovery paper by Hebb et al.[7] (2009) indicates an eccentricity of $e = 0.049^{+0.015}_{-0.015}$ derived from observations using the SOPHIE spectrograph, and a ground based z'-band occultation observation done by Lopez-Morales et al.[16] (2010) reports an occultation phase of $\phi = 0.5100^{+0.0072}_{-0.0061}$, both of which support the tidal heating model for explaining the size of WASP-12b. These results are disputed by Husnoo et al.[8] (2010) and Campo et al.[2] (2010) who have done new radial velocity measurements using the SOPHIE spectrograph ($e = 0.017^{+0.015}_{-0.011}$) and two occultation observations using the Spitzer Space Telescope ($\phi = 0.5012 \pm 0.0006$ and $\phi = 0.5007 \pm 0.0007$) respectively, which is consistent

with a circular orbit or a much smaller eccentricity than reported by Hebb et al.[7] (2009) and Lopez-Morales et al.[16].

This paper presents high-precision photometry of transits as well as occultations of WASP-12, aimed at providing more insight on the nature of the exoplanetary system. Section 2 describes the observations and the data reduction. The analyses and results are presented in Section 3. The findings are then discussed in Section 4 and the conclusions are summarized Section 5.

2 Observations and Reduction

Photometric observations of the 11.7th magnitude star WASP-12 [RA(J2000)=06:30:32.794, Dec(J2000)=+29:40:20.29] were conducted from late 2008 to early 2010 using the 1.2m telescope at the Fred Lawrence Whipple Observatory (FLWO) on Mount Hopkins in Arizona and the 2.56m Nordic Optical Telescope (NOT), operated on the island of La Palma jointly by Denmark, Finland, Iceland, Norway, and Sweden, in the Spanish Observatorio del Roque de los Muchachos Institutio Astrofisica de Canarias.

2.1 Observations at the FLWO

The data was collected using KeplerCam at the FLWO, which is a 4096×4096 pixel Fairchild 486 back-illuminated CCD which gives a $23.1' \times 23.1'$ field of view (FOV, see Figure 1). A 2×2 binning was used which reduced the readout and reset time to 11.5 s per frame and the typical readout noise was 7 e^- per binned pixel. The observations were made with both Sloan i' and z' filters. Autoguiding was used to make the image registration as constant as possible. Dome flats and zero-second (bias) frames were taken every night.

2.2 Observation at the NOT

The instrument used in the NOT observation was ALFOSC, which is owned by the Instituto de Astrofisica de Andalucia (IAA) and operated at the Nordic Optical Telescope under agreement between IAA and the NBIfAFG of the Astronomical Observatory of Copenhagen. ALFOSC is a 2048×2048 pixel CCD. It has as FOV of $6.4' \times 6.4'$ or 0.19" per pixel. The instrument was used in windowed fast-photometry mode, which means that only a specific region of the CCD containing WASP-12 and 3 nearby comparison stars of similar brightness was used and read-out. This mode reduced the readout time to 25 s from the original 90 s (see Figure 2). The typical readout noise was 3.2 e^- per pixel and the gain was 0.726 e^- per ADU. Zero-second images (bias) and sky flats were taken after the observation. A Johnson V filter was used. The night was photometric and data was collected well before and after predicted transit. The telescope was mildly de-focused to reduce pixel-to-pixel sensitivity variations and allow for longer exposure time. The autoguiding couldn't be fully maintained due to purely mechanical reasons when the target passed through the zenith in the second half of the observation. The exposure time was changed from 10 s to 9 s mid-observation to avoid saturation.

See Table 1 for details on the individual observations.

2.3 Data Reduction

No CCD instrument is perfect. Each pixel has a different sensitivity to light and zero-point value (bias). The bias difference can be compensated for by subtracting the science images with a zero-length exposure (bias frame), which suffers from the same drawbacks as the scientific images. The differences in sensitivity can be evened out by dividing the de-biased images with an exposure of an uniformly illuminated surface, for example the twilight sky or an artificial uniform light source inside the dome. This flat-fielding also partially compensates

ID	Date	Predicted HJD (mid)	Epoch	Event	Band	Exp. Time (s)
1	2008 Dec 18	2454820.03166±0.00088	285	Transit	z'	75
2	2008 Dec 20	2454821.66879±0.00088	286.5	Occultation	z'	75
3	2009 Jan 8	2454840.76869±0.00093	304	Transit	i'	40
4	2009 Jan 14	2454846.77152±0.00095	309.5	Occultation	i'	40
5	2009 Jan 15	2454847.86294±0.00095	310.5	Occultation	i'	40
6	2009 Jan 18	2454850.59150±0.00096	313	Transit	z'	90
7	2009 Jan 19	2454851.68292±0.00096	314	Transit	z'	60
8	2009 Feb 18	2454881.69705±0.0010	341.5	Occultation	i'	40
9	2009 Mar 2	2454893.70271±0.0011	352.5	Occultation	i'	40
10	2009 Mar 7	2454898.61411±0.0011	357	Transit	z'	75
11	2009 Mar 14	2454905.70836±0.0011	363.5	Occultation	z'	75
12	2009 Dec 6	2455172.56128±0.0018	608	Transit	V	10,9
13	2010 Jan 12	2455209.66967±0.0019	642	Transit	z'	60
14	2010 Jan 24	2455221.67532±0.0020	653	Transit	z'	120
15	2010 Jan 25	2455222.76674±0.0020	654	Transit	z'	120
16	2010 Feb 18	2455246.77805±0.0020	676	Transit	z'	150
17	2010 Mar 1	2454257.69228±0.0021	686	Transit	z'	75

Table 1: Dates of the observations with the predicted time of mid-eclipse with 1σ uncertainties using the ephemeris given by Hebb et al.[7] (2009), $T_0 = 2454508.9761^{+0.0002}_{-0.0002}$ days, $P = 1.091423^{+0.000003}_{-0.000003}$ days. Times for occultations assumes a circular orbit.

for optical obstructions, such as dust or vignetting. To achieve better calibration, many calibration images are taken and are then average combined into a master-bias and a master-flat, which is then used in the final calibration.

The data from KeplerCam was overscan corrected, de-biased and flat-fielded using standard calibration routines in *IRAF* and the ALFOSC data was similarly calibrated using *MaximDL*. All the calibrated datasets were examined using DS9 and 11 and 3 comparison stars with a brightness within a factor of 2 to WASP-12 were chosen to be part of the next step in the reduction for the FLWO and NOT datasets respectively. DAOPHOT-type aperture photometry was performed in each frame of each observation. Apertures ranging from 4 to 19 pixels were tried on order to find the one that produced the highest signal-to-noise ratio in the out-of-transit (OOT) data. The underlying flux contribution from the sky was

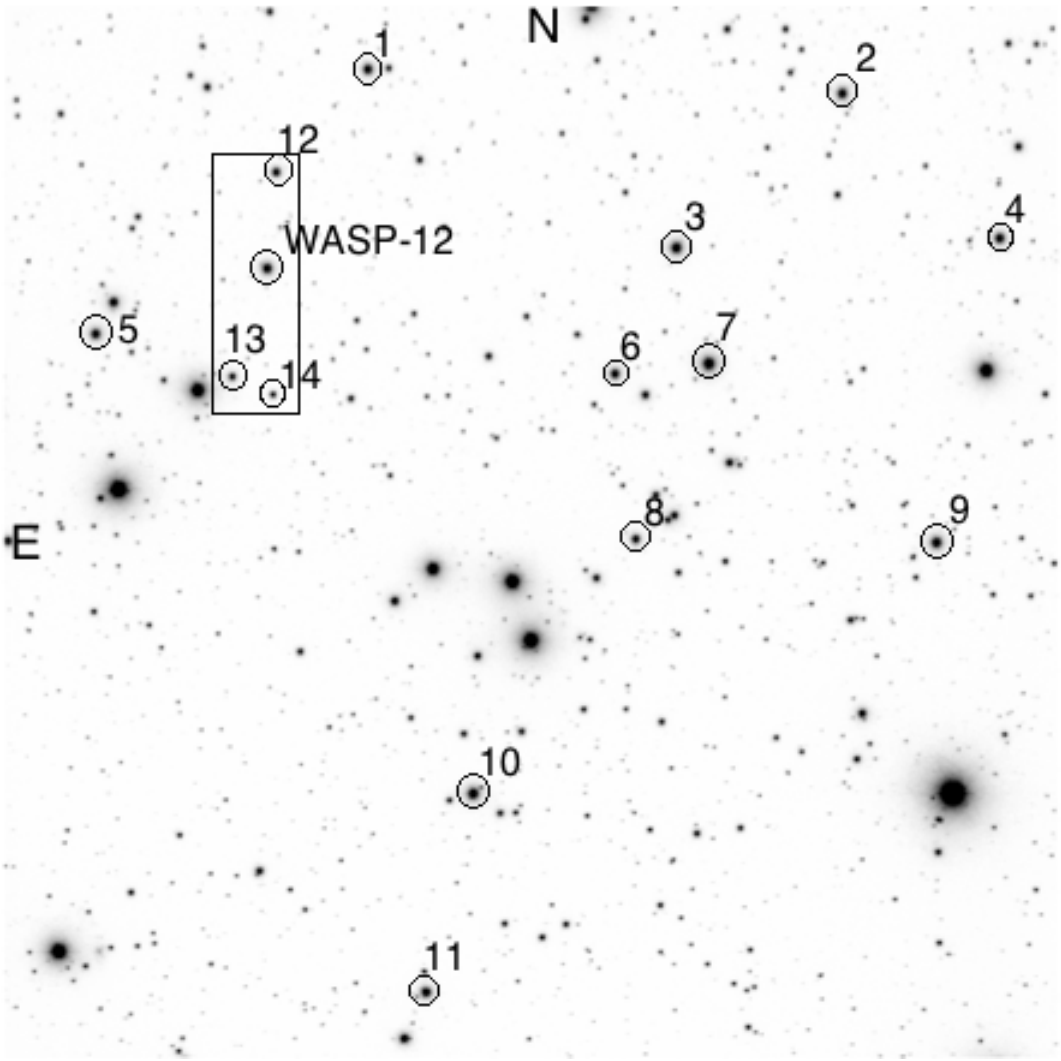

Figure 1: KeplerCam FOV.

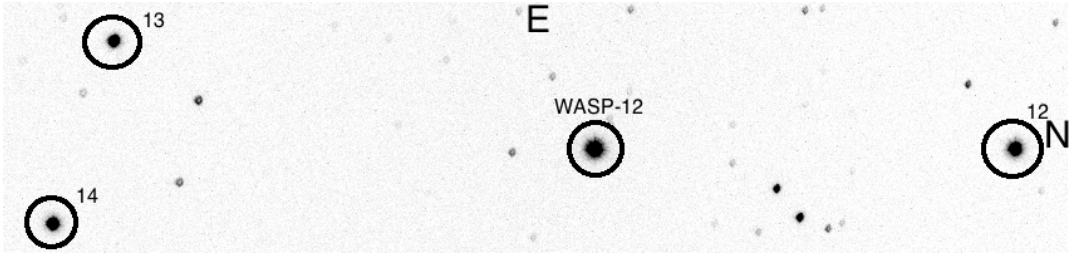

Figure 2: ALFOSC windowed FOV

subtracted after estimating its brightness within an annulus centered on each star ranging from 40 to 50 pixels in radius.

The *Interactive Data Language* (IDL) was from here on used for the rest of the reduction and analysis. Careful differential photometry was performed for all individual datasets. The flux of each comparison star was combined into a comparison signal, with which the flux of the target was to be divided by. The individual weight of each comparison star's flux in the comparison signal was set proportional to σ^{-2}, where σ is the standard deviation of the star's mean flux. Weighing by σ^{-1}, $\sigma^{-1/2}$ and 1 (flat weightening) was also tried, but proved to be less effective. Thereby stars with a more constant flux and high signal-to-noise was favored in the comparison signal. Comparison stars with obvious flaws, for example behaving differently to variations in airmass due to differences in color, were not included in the reference signal. Many other configurations of comparison stars included in the comparison signal were tried, including such when comparison stars without any obvious flaws were excluded. The flux of the target was then divided by the final comparison signal and corrected for airmass variations by dividing the relative flux by an exponential function of airmass. The parameters of the exponential function was optimized by fitting the OOT data.

The uncertainty of the photometry was computed from the quadrature sum of the errors due to Poisson noise in all the stars used in the final differential photometry, the Poisson noise from the sky background, the readout noise from the CCD detector and the scintillation noise calculated using the empirical formulas given in Young[24] (1967) and Dravins[6] (1998). The dominant term is the Poisson noise from WASP-12.

See Table 2 for details on the individual observations.

ID	Ap.	Comp. stars	Excluded data (HJD - constant)	OOT RMS (10^{-4})	σ/σ_t
1	8	1,5,11	.055-.10	20	2.35
2	13	1,5,11	.60-.65	11	1.38
3	7	1,3,5,8,10	-	18	2.03
4	13	1,3,5,8,10	-	14	1.59
5	14	1,3,5,8,10	-	10	1.29
6	13	1,5,11	.69-.72	19	-
7	11	1,5,11	.55-.617	11	1.15
8	16	1,3,5,8,10	.06-.066	11	1.22
9	11	1,3,5,8,10	-	16	1.59
10	6	1,5,11	-	12	1.36
11	12	1,5,11	.6-.667	17	1.52
12	18	12,13,14	.61-.623	11	1.30
13	6	1,5,11	.615-.64,.71-.75	20	1.36
14	12	1,5,11	.71-.75	31	1.78
15	5	1,5,11	-	23	3.08
16	8	1,5,11	.82-.95	18	2.29
17	6	1,5,11	-	49	2.46

Table 2: Data lost to clouds or high airmass was excluded from subsequent analysis (Column 4). The OOT RMS is the standard deviation of all points out-of-transit and the last column gives the ratio between the measured noise in the data and the theoretical noise.

3 Analysis and Results

When the light curves were done, the determination of stellar, planetary and orbital parameters for the system WASP-12 began. Two methods were used to determine the parameters and their uncertainties. The first was the least χ^2 method using the AMOEBA algorithm (Press et al.[19] 1992) in IDL, which is based on the downhill simplex method of Nelder and Mead[18] (1965), to constrain single parameters for some of the occultation light curves where only one parameter was fitted, or to obtain initial values for the cases when several parameters needed to be fitted. The second method, used to derive the parameters and uncertainties in the multi-parameter fits, was a Markov Chain Monte Carlo (MCMC) algorithm. Tegmark et al.[23] (2004) elaborates more on the astrophysical applications of the MCMC.

3.1 Transits

The transit light curves were critically studied individually and only the curves of sufficient quality were used in the final analysis. Many light curves had no or very little data OOT, only data on part of the transit or very high OOT RMS. The dataset from January 8, 2009, (ID[3]) produced by the FLWO and the dataset from December 6, 2009, (ID[12]) produced by the NOT were the only datasets left after this step.

The geometry of photometric transits has been studied in great detail by Mandel & Agol[14] (2002). Their analytic formulas together with quadratic limb darkening law with coefficients from Claret[4][5] (2000, 2004) was used in the MCMC transit simulations ($u_1 = 0.7404, u_2 = 0.2979$ for V-band and $u_1 = 0.1415, u_2 = 0.3709$ for z'-band). An eleven parameter MCMC algorithm was used to analyze the two datasets globally. The parameters fitted were $\{tc_1, tc_2, b, p^2, R_\odot/a, a_1, a_2, a_3, a_4, u_1, u_2\}$, where tc_1 and tc_2 are the times of mid-transit, b is the impact parameter, p^2 is the star-planet area ratio squared, $R_\odot/a$ is the stellar radius-orbital semimajor axis ratio, a_1 to a_4 are the airmass correction parameters and the u_1 and u_2 are the first limb darkening coefficients for the z'-band and V-band respectively. A chain with 7×10^6 links was produced and parameters with uncertainties were obtained. See Table 3 for the resulting parameters and Figure 3 for the plotted best-fit light curve from the MCMC.

A new ephemerides was calculated by fitting a linear function with two degrees of freedom to the FLWO data, the NOT data and two times of mid-transit from the WASP-team published in Table 2 of Campo et al.[2] (2010). The χ^2 of the fit was equal to 4.20. See table 4 for the new Epoch and Period and Figure 4 for the O-C diagram.

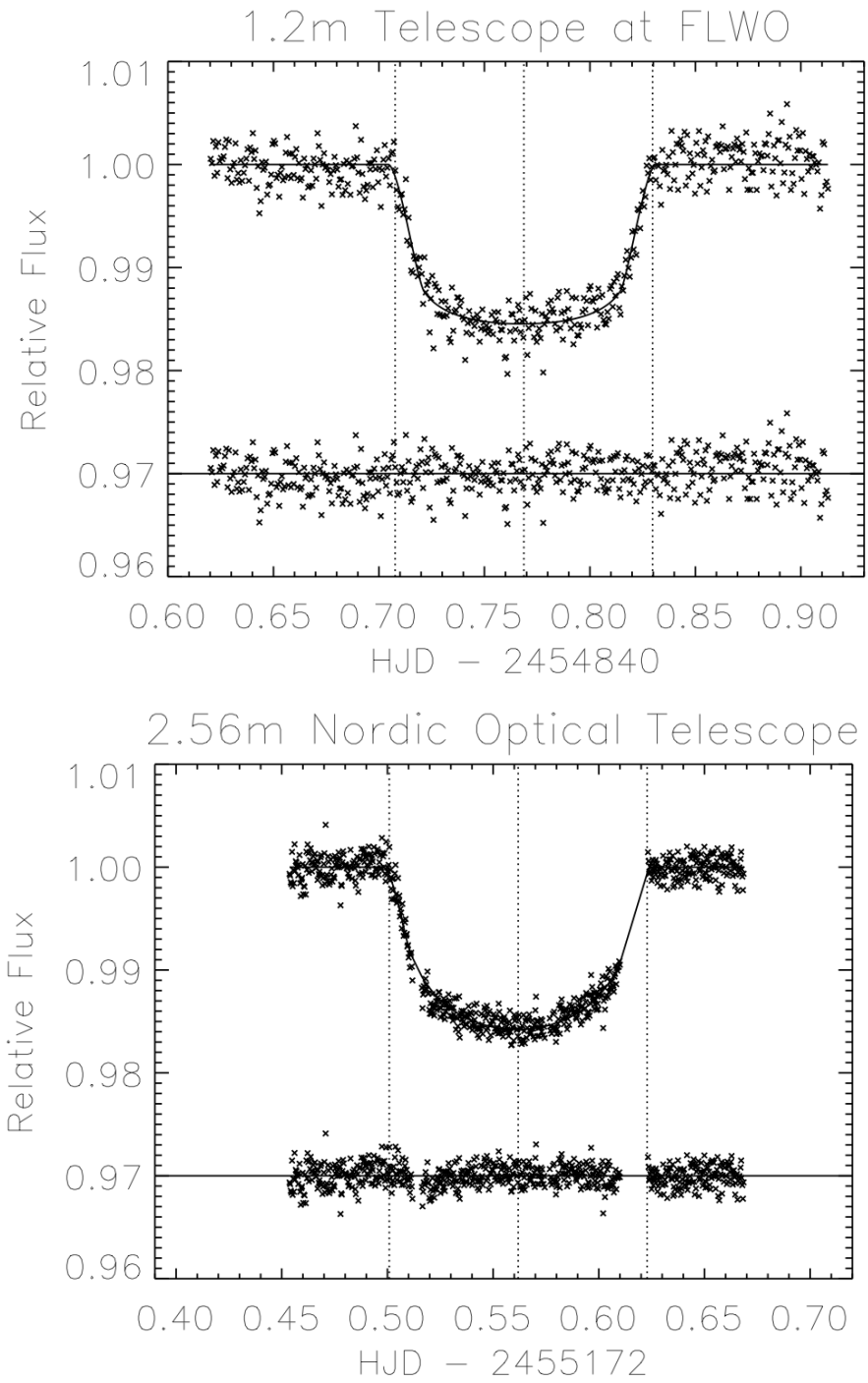

Figure 3: Upper: FLWO transit with residuals. Lower: NOT transit with residuals. The overplotted dashed lines illustrates the predicted times for ingress, mid-transit and egress.

Parameter	Symbol	Value	Unit
Planet/star area ratio	$(R_p/R_s)^2$	$0.0129^{+0.0004}_{-0.0004}$	
Transit duration	t_T	$0.1276^{+0.0016}_{-0.0014}$	days
Impact parameter	b	$0.33^{+0.10}_{-0.17}$	R_*
Orbital semimajor axis	a	$0.0229^{+0.0008}_{-0.0008}$	AU
Stellar/semimajor axis radius ratio	R_*/a	$0.366^{+0.013}_{-0.012}$	
Inclination	i	$83.6^{+3.4}_{-2.2}$	degrees
Stellar radius	R_*	$1.65^{+0.08}_{-0.08}$	$R_\odot$
Planet radius	R_p	$1.82^{+0.12}_{-0.10}$	R_j
Planet mass	M_p	$1.40^{+0.10}_{-0.10}$	M_j
Planet density	ρ_p	$0.22^{+0.03}_{-0.02}$	ρ_j
Time of mid-transit FLWO	$t_{mid-FLWO}$	$2454840.76782^{+0.00031}_{-0.00031}$	HJD
Time of mid-transit NOT	$t_{mid-NOT}$	$2455172.56097^{+0.00031}_{-0.00027}$	HJD
First limb darkening coefficient	$u_{1i'-band}$	$0.436^{+0.067}_{-0.067}$	
First limb darkening coefficient	$u_{1V-band}$	$0.538^{+0.034}_{-0.033}$	

Table 3: WASP-12 system parameters derived from MCMC analysis. Quoted values are medians and the uncertainties are 16% and 84% levels of cumulative distribution. The values of R_j and M_j were derived using $K_1 = 226 \pm 0.004$ m s^{-1} and $M_* = 1.35 \pm 0.14 M_\odot$ from Hebb et al.[7] (2009).

Parameter	Symbol	Value	Unit
Transit epoch (HJD)	T_0	$2454508.97606 \pm 0.00012$	days
Orbital period	P	1.0914221 ± 0.0000005	days

Table 4: New ephemerides with 1σ uncertainty from a linear fit with two degrees of freedom.

3.2 Occultations

Bad data was sorted from the occultation data sets using a method similar to the method used on the transit light curves. All the i'-band observations (ID [4], [5], [8] and [9]) were selected to be part of the final analysis. See Figure 5 for the light curves and a composite of all i'-band occultation observations.

3.2.1 Assuming $e = 0$

The AMOEBA algorithm was used to constrain the depth of the occultation. The duration and times of mid-occultation were fixed to the predicted values assuming a circular orbit.

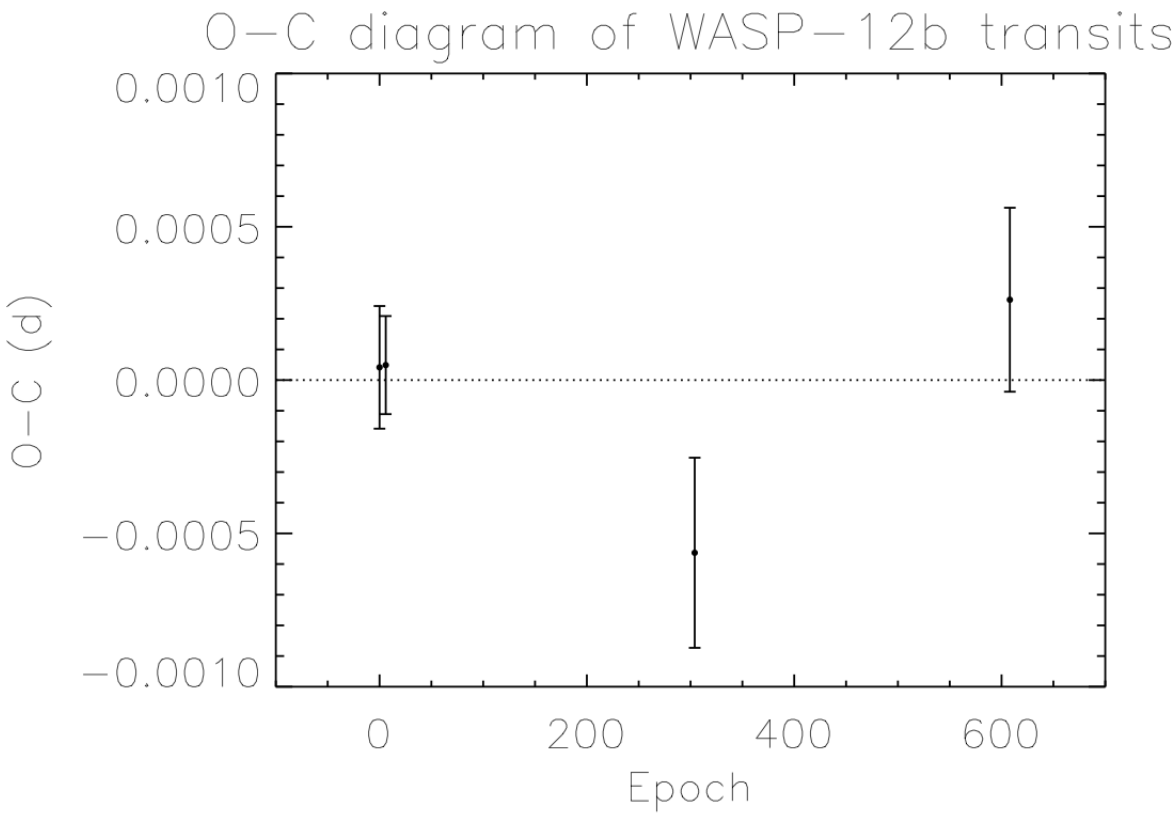

Figure 4: Observed time of mid-transit subtracted by the calculated time of mid-transit (O-C). The two earlier points come from the WASP-team and were published in Table 2 of Campo et al.[2] (2010).

The effect of limb darkening on the occulted planet was neglected for having too small of an effect to be important for the purposes of this paper. The more observations stacked together, the higher signal-to-noise is achieved. Different configurations of which datasets to include in the analysis were tried to see if there was an observed occultation in all the datasets. Table 5 shows all possible combinations of included datasets and the result including uncertainties.

3.2.2 Allowing for $e \neq 0$

These analyses were done using a two-parameter MCMC algorithm with 5×10^5 links designed to constrain both the occultation depth and the time of mid-occultation. The period was

ID included	Depth in ppm (flux)	68.3% confidence	99.73% confidence	Depth/1σ error
4,5,8,9	400	$\pm$52	$\pm$160	7.7
5,8,9	490	$\pm$60	$\pm$180	7.3
4,8,9	480	$\pm$66	$\pm$200	7.3
4,5,9	250	$\pm$61	$\pm$180	4.1
4,5,8	400	$\pm$57	$\pm$170	7.0
4,5	210	$\pm$68	$\pm$210	3.1
4,8	490	$\pm$76	$\pm$230	6.4
4,9	250	$\pm$85	$\pm$260	2.9
5,8	500	$\pm$68	$\pm$210	7.5
5,9	320	$\pm$74	$\pm$230	4.3
8,9	700	$\pm$84	$\pm$250	8.3
4	120	$\pm$110	$\pm$330	1.1
5	260	$\pm$90	$\pm$270	2.9
8	850	$\pm$110	$\pm$320	7.8
9	450	$\pm$140	$\pm$420	3.2

Table 5: WASP-12b occultation depths in ppm with confidence intervals, fixing duration and time of mid-occultation according to the prediction assuming circular orbit. Details on which observations were included is given in the first column.

Parameter	Symbol	Value	Unit
Time of mid-occultation	t_c	$0.0201^{+0.0031}_{-0.0042}$	days
Epoch of mid-occultation	ϕ	$0.518^{+0.003}_{-0.004}$	phase
Bounds on e	$e\cos\omega$	$0.029^{+0.006}_{-0.005}$	
Occultation depth	δ	$0.00046^{+0.00005}_{-0.00005}$	flux

Parameter	Symbol	Value	Unit
Time of mid-occultation	t_c	$0.0188^{+0.0058}_{-0.0083}$	days
Epoch of mid-occultation	ϕ	$0.517^{+0.005}_{-0.008}$	phase
Bounds on e	$e\cos\omega$	$0.027^{+0.008}_{-0.013}$	
Occultation depth	δ	$0.00029^{+0.00006}_{-0.00006}$	flux

Table 6: Upper: WASP-12b parameters and 1σ error limits derived from MCMC analysis using all four i'-band observations of occultations. The predicted time of mid-occultation assuming a circular orbit was calculated using the ephemeris in Hebb et al.[7] (2009) and t_c is the measured deviation from that prediction. Lower: Same as upper but excluding the third dataset (ID[8]).

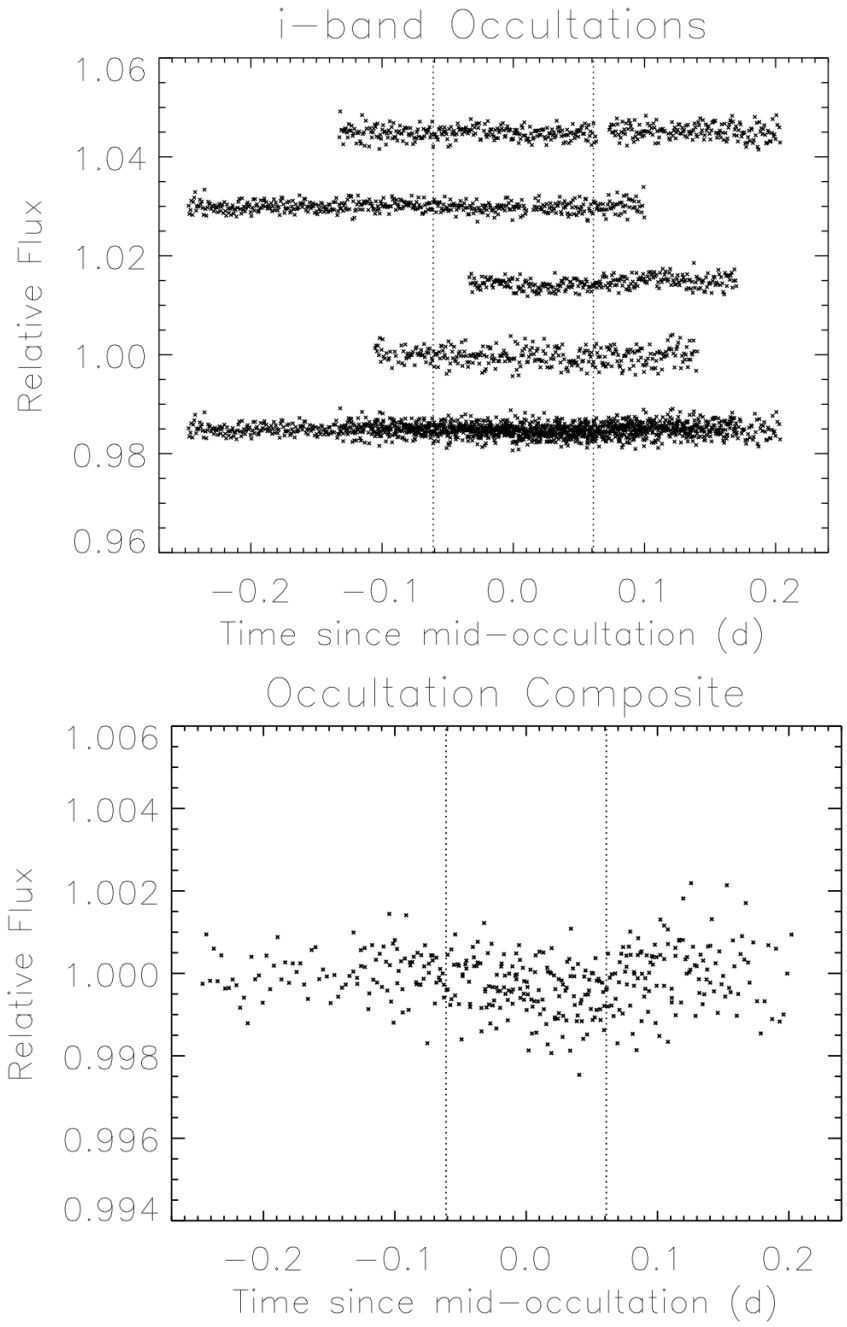

Figure 5: Upper: The four i'-band occultations with a composite of them all at the bottom. The observations are offset by 0.015 flux. Lower: The composite data of the four i'-band occultations, here binned with a bin size of four subsequent data points in each bin. The overplotted dashed lines illustrates the predicted times for ingress and egress assuming a circular orbit.

assumed to be constant, so the time between the occultations was kept fixed, but the time of mid-occultation was allowed to vary globally (Upper Table 6). Since the analysis in Section 3.2.1 showed an anomaly in the measured depth when the third dataset (ID[8]) was left out of the analysis, this was also done here to check whether a similar result would appear (Lower Table 6).

4 Discussion and Conclusions

WASP-12b continues to be a very special planet. The bloated radius reported in Hebb et al.[7] (2009) is confirmed ($1.82^{+0.12}_{-0.10}$ R_j) and is even slightly enlarged, but well within the uncertainty. It should be noted that the planet-star ratio ($(R_p/R_s)^2 = 0.0129^{+0.0004}_{-0.0004}$) derived from the MCMC analysis is smaller than the one reported by Hebb et al.[7] (2009), and that it is instead the larger stellar/semimajor axis radius ratio ($R_*/a = 0.366^{+0.013}_{-0.012}$) resulting from the longer measured duration of the transit ($0.1276^{+0.0016}_{-0.0014}$ days) that is responsible for the slightly larger estimated radius.

The ephemerides of WASP-12b was updated using the new transit data. The transit epoch (HJD) of $T_0 = 2454508.97606 \pm 0.00012$ days and orbital period of $P = 1.0914221 \pm 0.0000005$ days has almost one order of magnitude lesser uncertainty than the original one presented by Hebb et al.[7] (2009). It should be noted that the timing of the 6 December 2009 transit, obtained here using an MCMC algorithm, differs from the timing reported by the ETD website using the same data ($t_{mid-NOT} = 2455172.56097^{+0.00031}_{-0.00027}$ reported here and $t_{mid-NOT} = 2455172.5620^{+0.00014}_{-0.00014}$ reported on ETD). There is a possibility that the data obtained between third and forth contact, when the autoguiding was lost, is faulty, and it was therefore not included in the analysis of this paper. The data was however used in the analysis of the ETD website, and that possible bias might have contributed to an underestimated uncertainty or an incorrect timing altogether. The timing based on the value from ETD was

used in Campo et al.[2] (2010) to constrain a new ephemeris (see Table 2 and Figure 3 in Campo et al.[2] 2010), and that might have resulted in an incorrect determination of the new ephemeris in that paper.

The four i'-band observations of occultations proved to be interesting. A decrease in flux was observed in all datasets when the time of mid-occultation was fixed at its predicted value assuming a circular orbit, for most of them significant to a 3σ deviance from 0. When composed to increase the signal-to-noise ratio, the decrease in flux is even more certain and the probability of it originating from the occultation of WASP-12b is certain to the 9σ level. The difference between the $\delta = 0.00046 \pm 0.00005$ reported here and the $\delta = 0.00082 \pm 0.00015$ reported by Lopez-Morales et al.[16] (2010) can be explained by the use of an i'-band filter here and z'-band filter in Lopez-Morales et al.[16] (2010). The fact that these observations were made in a shorter wavelength is, together with the z'-band observations published by other authors, of interest when modeling the atmospheric characteristics of WASP-12b (Lopez-Morales et al.[16] 2010).

The result of the MCMC analysis when the epoch of mid-occultation was allowed to vary globally is even more interesting. The time of mid-occultation did not change considerably when the third dataset (ID[8]) was left out of the analysis and a small offset is observed from the predicted time assuming a circular orbit ($\phi = 0.518^{+0.003}_{-0.004}$). The timing obtained in this paper and the timing reported by Lopez-Morales et al.[16] (2010) ($\phi = 0.5100^{+0.0072}_{-0.0061}$) is consistent and the resulting eccentricity is consistent with the one reported by Hebb et al. (2009). But even though the timing of the occultations suggest a small orbital eccentricity, consistent with that found by other authors, the timing is very uncertain and continued precise photometric monitoring of transits and occultations of WASP-12b is necessary to further constrain the true eccentricity of the orbit of WASP-12b.

As discussed in Section 1, the orbit should circularize due to tidal effects (Rasio et al.[20] 1996). However, this paper confirms the eccentricity and thus allows for the large

radius of WASP-12b to be explained by tidal heating effects (Ibgui et al.[9] 2010; Miller, Fortney & Jackson[17] 2009). Orbital precession could also be present and observable through timing of the transits and occultations (Campo et al.[2] 2010). Possible explanations to the eccentric orbit include the presence of a gravitationally interacting 3rd body, a several orders of magnitude higher value of the tidal dissipation constant Q_P, or that the system is much younger than estimated and haven't had time to circularize yet. Future observations and analyses are needed to prove which model best explains the special case of WASP-12b.

5 Acknowledgments

I would like to thank Prof. Joshua N. Winn at the Department of Physics and the Kavli Institute for Astrophysics and Space Research at the Massachusetts Institute of Technology, whose great mentorship and expertise has been of utmost importance for this research. Many great thanks goes to Mr. Roberto Sanchis for always providing help and support when needed. I would also like to thank my tutor Dr. John Rickert, whose helpful suggestions has greatly improved this paper. My final thanks goes to the Center for Excellence in Education and Kjell och Märta Beijers Stiftelse for making this research possible.

References

[1] A. Burrows, I. Hubeny, J. Budaj, W. B. Hubbard. Possible Solutions to the Radius Anomalies of Transiting Giant Planets. The Astrophysical Journal, no. 661, 502–514.

[2] C. J. Campo, J. Harrington, R. A. Hardy, K. B. Stevenson, S. Nymeyer, D. Ragozzine, N. B. Lust, D. R. Anderson, A. Collier-Cameron, J. Blecic, C. B. T. Britt, W. C. Bowman, P. J. Wheatley, D. Deming, L. Hebb, C. Hellier, P. F. L. Maxted, D. Pollaco, R. G. West. On the Orbit of Exoplanet WASP-12b. Submitted to The Astrophysical Journal (2010).

[3] D. Charbonneau, T. M. Brown, D. W. Latham, M. Mayor. Detection of Planetary Transits Across a Sun-like Star. The Astrophysical Jornal Letters (2000), no. 529, 45–48.

[4] A. Claret. Non-linear Limb-darkening Law for LTE Models. Astronomy and Astrophysics (2000), no. 363, 1081–1190.

[5] A. Claret. Non-linear Limb-darkening Law for LTE Models. III. Astronomy and Astrophysics (2004), no. 428, 1001–1005.

[6] D. Dravins, L. Lindegren, E. Mezey and A. T. Young. Atmospheric Intensity Scintillation of Stars. Publications of the Astronomical Society of the Pacific (1998), no. 110, 610.

[7] L. Hebb, A. Collier-Cameron, B. Loeillet, D. Pollacco, G. Hbrard, R. A. Street, F. Bouchy, H. C. Stempels, C. Moutou, E. Simpson, S. Udry, Y. C. Joshi, R. G. West, I. Skillen, D. M. Wilson, I. McDonald, N. P. Gibso, S. Aigrain, D. R. Anderson, C. R. Ben, D. J. Christia, B. Enoc, C. A. Haswell, C. Hellier, K. Horn, J. Irwin, T. A. Lister, P. Maxted, M. Mayor, A. J. Norton, N. Parley, F. Pont, D. Queloz, B. Smalley, P. J. Wheatley. WASP-12b: The Hottest Transiting Extrasolar Planet Yet Discovered. The Astrophysical Journal (2009), no. 693, 1920–1928.

[8] N. Husnoo, F. Pont, G. Hebrard, E. Simpson, T. Mazeh, F. Bouchy, C. Moutou, L. Arnold, I. Boisse, R. Diaz, A. Eggenberger, A. Shporer. Orbital Eccentricity of WASP-12 and WASP-14 from New Radial-velocity Monitoring with SOPHIE. Monthly Notices of the Royal Astronomical Society (2010).

[9] L. Ibgui, A. Burrows and D. S. Spiegel. Tidal Heating Models for the Radii of the Inflated Transiting Giant Planets WASP-4b, WASP-6b, WASP-12b, WASP-15b, and TrES-4. The Astrophysical Journal (2010), no. 713, 751–763.

[10] J. Kallrath and E. F. Milone. *Eclipsing Binary Stars : Modeling and Analysis*. Springer-Verlag (1999).

[11] H. A. Knutson, D. Charbonneau, R. W. Noyes, T. M. Brown, R. L. Gilliland. Using Stellar Limb-Darkening to Refine the Properties of HD 209458b. The Astrophysical Journal, no. 655, 564–575.

[12] D. Lai, C. Helling, E.P.J. van den Heuvel. Mass Transfer, Transiting Stream and Magnetopause in Close-in Exoplanetary Systems with Applicatons to WASP-12. Submitted to The Astrophysical Journal (2010).

[13] S. Li, N. Miller, Douglas N.C. Lin, J. J. Fortney. WASP-12b as a Prolate, Inflated and Disrupted Planet from Tidal Dissipation. Nature (2010), no. 463, 1054–1056.

[14] K. Mandel and E. Agol. Analytic Light Curves for Planetary Transit Searches. The Astrophysical Journal (2002) no. 580, 171–175.

[15] M. Mayor, D. Queloz. A Jupiter-mass Companion to a Solar-type Star. The Astrophysical Journal (1995), no. 378, 355–359.

[16] M. Lopez-Morales, J. L. Coughlin, D. K. Sing, A. Burrows, D. Apai, J. C. Rogers, D. S. Spiegel, E. R. Adams. Day-side z'-band Emission and Eccentricity of WASP-12b. The Astrophysical Journal (2010), no. 716, 36–40.

[17] N. Miller, J.J. Fortney, B. Jackson. Inflating and Deflating Hot Jupiters: Coupled Tidal and Thermal Evolution of Known Transiting Planets. The Astrophysical Journal (2009), no. 702, 1413–1427.

[18] J. A. Nelder and R. Mead. A Simplex Method for Function Minimization. Computer Journal (1965), Vol 7, 308–313.

[19] W. H. Press,S. A. Teukolsky, W. T. Vetterling and B. P. Flannery. *Numerical recipes in C. The art of scientific computing*. Cambridge: University Press, 1992, 2nd ed.

[20] F. A. Rasio, C. A. Tout, S. H. Lubow, M. Livio. Tidal Decay of Close Planetary Orbits. The Astrophysical Journal (1996), no. 470, 1187–1191.

[21] J. Southworth, P. J. Wheatley and G. Sams. A Method for the Direct Determination of the Surface Gravities of Transiting Extrasolar Planets. Monthly Notices of the Royal Astronomical Society: Letters, Vol. 379, 11–15.

[22] J. N. Winn. Chapter *Transits and Occultations* in *EXOPLANETS*, ed. S. Seager. University of Arizona Press (in press).

[23] M. Tegmark, M. Strauss, M. Blanton, K. Abazajian, S. Dodelson, H. Sandvik, X. Wang, D. Weinberg, I. Zehavi, N. Bahcall, F. Hoyle, D. Schlegel, R. Scoccimarro, M. Vogeley, A. Berlind, T. Budavari, A. Connolly, D. Eisenstein, D. Finkbeiner, J. Frieman, J. Gunn, L. Hui, B. Jain, D. Johnston, S. Kent, H. Lin, R. Nakajima, R. Nichol, J. Ostriker, A. Pope, R. Scranton, U. Seljak, R. Sheth, A. Stebbins, A. Szalay, I. Szapudi, Y. Xu and 27 others (the SDSS collaboration). Cosmological parameters from SDSS and WMAP. Physical Review D (2004).

[24] A. T. Young. Photometric error analysis. VI. Confirmation of Reiger's theory of scintillation. The Astronomical Journal (1967), no. 72, 747.